

# Exudates Detection for Multiclass Diabetic Retinopathy Grade Detection using Ensemble

Farrikh Alzami<sup>1</sup>, Rama Aria Megantara<sup>1</sup>, Abdussalam<sup>1</sup>, Purwanto<sup>1</sup>, Ahmad Zainul Fanani<sup>1</sup>, Pulung Nurtantio Andono<sup>1</sup>, Moch Arief Soeleman<sup>1</sup>

Dept. of Computer Science, Universitas Dian Nuswantoro, Semarang, Indonesia<sup>1</sup>



**Abstract**— Long term diabetes could cause the diabetic retinopathy (DR) disease, if in long term is not treated appropriately, could affect in loss of vision and the effect is irreversible. Automated DR grading is important to help the ophthalmologist in DR treatment. Exudates detection is part of DR detection, but unfortunately, the exudates detection mostly focusses on binary grading (disease or no disease) rather than multi-class grading. Thus, in this paper, we proposed method in multiclass DR detection by using exudates candidates. Exudates candidates can be obtained by utilized CLAHE and wiener filter to enhanced the fundus images. Then to improve the candidates, region growing, segmentation and clustering methods which considering circularity, areas and eccentricity are utilized. Finally, Those candidates were extracted for features using statistical features and fed into ensemble learning process. The results concluded that our methods with XG-Boost as ensemble classifier is able to grade the multi-class DR severity level and comparable with other researcher which use MESSIDOR datasets.

**Keywords**— diabetic retinopathy, ensemble learning, exudates detection, MESSIDOR, IDRiD

## 1. Introduction

Shaw et.al estimates 360 million people suffered from diabetes in 2010 and increase to 439 million in 2030 (Shaw, Sicree, & Zimmet, 2010). Long term diabetes could cause the diabetic retinopathy (DR) disease. If DR in long term is not treated appropriately, could affect in loss of vision and the effect is irreversible. Thus, automated DR screening is important to detect the first sign of DR disease especially for developing countries where the ophthalmologists is not available in many areas. Automated DR screening could help the ophthalmologist in DR detection to support the DR evidence, resulted that the DR disease could be handled and treated immediately. According to Mookiah et.al (Mookiah et al., 2013) DR can be detected by several characteristics: Exudates, which caused by blood leakages from veins; Hemorrhages (HMA) which caused by blood leakages from damaged capillaries; and Microaneurysms (MA) is the deformations in walls of blood vessels. According to Fleming et.al (Fleming et al., 2010), the exudates and hemorrhages detection gave increase in the performance of DR without affecting manual grading workload. Abramoff et.al (Abramoff et al., 2010) also stated the importance of exudates detection in DR grading. Ensemble learning also gaining popularity in medical fields, such as epileptic seizure (Hosseini, Pompili, Elisevich, & Soltanian-Zadeh, 2018) (Alzami et al., 2018) (Mursalin, Zhang, Chen, & Chawla, 2017), Arrhythmia (G. Chen, Hong, Guo, & Pang, 2019) (Mondéjar-Guerra, Novo, Rouco, Penedo, & Ortega, 2019), not exceptionally in diabetic retinopathy classification, such as; Antal and Hajdu (Antal & Hajdu, 2014) which using ensemble learning in both image processing and decision making; Zhang et.al (Zhang et al., 2014) using random forest in exudates decision making; Alzami et.al (Alzami, Abdussalam, Megantara, Fanani, & Purwanto, 2019) using random forest fed by fractal analysis to obtain the DR grading; and Fraz et.al (Fraz, Jahangir, Zahid, Hamayun, & Barman, 2017) using bagging for exudates classification whereas ground truth will be used as training. Research in DR detection, either in public dataset such as MESSIDOR, IDRiD or private dataset, mostly focus on disease or no disease classification (binary class grading) (Niemeijer, Abramoff, & van Ginneken, 2009) (Antal & Hajdu, 2014) (Figueiredo, Kumar, Oliveira, Ramos, & Engquist, 2015a) (Harangi & Hajdu, 2014), rather than multi-class grading which means the multi class grading is not fully explored (Usman Akram, Khalid, Tariq, Khan, & Azam, 2014). Fleming et.al (Fleming et al., 2010) also stated that disease - no disease state can be performed using microaneurysm detection and image quality assessment, but the disease grading need handling with more efforts. Thus, in this research, we focus on multi class DR grading using exudates detection where we believe it have room for improvement.

In this paper, we presented diabetic retinopathy classification based on severity grade using exudates detection. By using wiener filter and CLAHE to enhanced the fundus images, region growing, segmentation and clustering which considering circularity, areas and eccentricity to obtain the exudates candidates, several statistical features were extracted from exudates candidates, then several ensemble methods were used to find which classifier is able to grade the severity of DR. From the conducted experiments, the methods obtained high performance and comparable with other researchers. The rest of paper is organized as follows: section 2 briefly describes about related works, especially in exudates detection; section 3 explains about the methods we are utilized; results, effect and discussion from the methods are described in section 4; finally, section 5 presents our conclusion and propose the future works.

## 2. Related Work

One of exudates detection methods, fall in region growing and pattern recognition methods. In region growing approach, several researchers proposed methods as follows: Li and Chutatape (Li & Chutatape, 2004) proposed optic disk detection by using modified active shape model and principal component analysis, then exudates detection by combined edge detection and region growing; Cardenas et.al (Cárdenas, Martinez-Perez, March, & Hevia-Montiel, 2013) proposed mean-shift filtering to uniform background non-structures regions and enhance bright areas, then the local maxima regions were used as seeds to perform the region growing. In pattern recognition categories, several researcher proposed methods to obtain exudates as follows: Figueiredo et.al (Figueiredo et al., 2015a) proposed lesion detection using wavelet and hessian multiscale analysis which produced multiscale features, then fed into binary classifier. the proposed method obtains satisfactory results, but lack of description about the classifier and the parameter was used; Liu et.al (Liu et al., 2017) proposed exudates detection in several steps, such as matched filter based on vessel segmentation and saliency based optic detection is used to remove the vessel and optic. Then random forest is used to classify exudate-free patches and exudate patches.

In our research, we taking part in region growing and pattern recognition approach. This research explores the effect of using wiener filter and CLAHE as fundus image enhancement method; image normalization is placed in crucial step; region growing segmentation and clustering process to obtain the exudates candidates; statistical features were extracted from exudates candidates; then ensemble learning such as Random Forest, META-DES and XG-Boost is used as multi-class DR severity level classification.

## 3. Methods

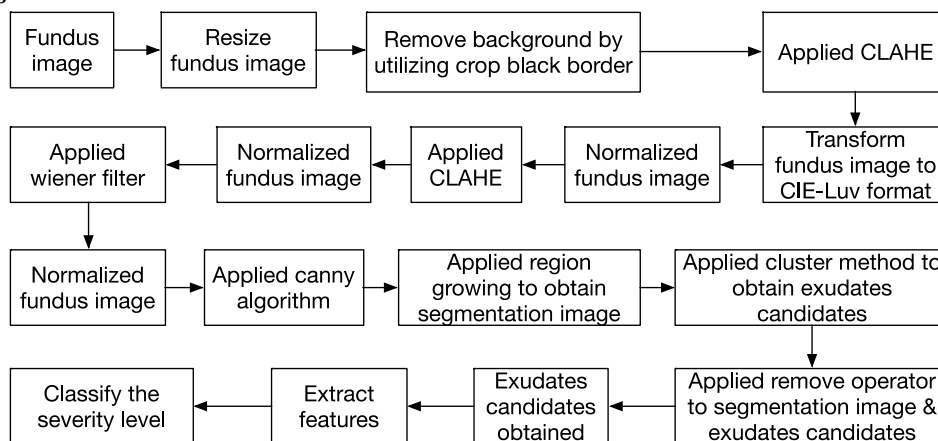


Figure 1: Multi-class DR grade classification approach

Our methods can be summarized in figure 1 and described as following steps: **First step** is image preprocessing step: In here, we load and resize the fundus image which help to reduce the computation while maintaining the fundus images quality. Then, we need to remove background with our fundus image by utilizing crop black border methods. In here, 3 is used as threshold (ztol) to differentiate the background and fundus images. Next, Contrast Limited Adaptive Histogram Equalization (CLAHE) which described in (Pizer et al., 1987) is used as image enhancements. **Second step** is exudates detection: After the fundus images already enhanced using CLAHE, the next step is detecting the exudates candidates. First, we convert those

enhanced fundus images into CIE luv color space. The reason CIE luv is used is due to fundus images illumination is not uniform. Then, the CIE luv fundus images were normalized to ensure each pixel has similar data distribution which help to reduce the overhead computation. The normalized CIE luv are enhanced again using CLAHE. To ensure the enhanced images still have same data distribution, the enhanced images were normalized once again. Second, wiener filter was performed to remove excessive noise from enhanced fundus images. Then, those noise free fundus images were normalized. Third, canny algorithm was applied as edge filter for normalized fundus images. In here, we used 3 as standard deviation of the gaussian filter. Fourth, region growing was applied to normalized fundus images with the edges values is fed from the canny algorithm calculation. The reason we chose region growing due to region growing are able to separate the regions that have same characteristics, resulted in clear segmentation results (segmentation image). Finally, we utilized clustering methods by considering several cluster parameters, such as: circularity, areas and eccentricity from segmentation results to obtain the exudates candidates. The value for circularity we set to more than 0.05, areas more than 10 and less than 1000, eccentricity more than 0.1. detailed explanation about clustering parameters are describes as follows: let assume the images have dimension as  $m \times n$ , in here, **cluster areas** are obtained using region props method; to obtain **circularity**, first me must find the boundaries of images and set as **borders**, then we calculate the **cluster perimeters** as follows:

Algorithm 1: cluster perimeters
input  Segmentation image as <b>sgm_img</b> with dimension $m \times n$
Ensure  1 Number_cluster = max value from <b>sgm_img</b> array object + 1  2 Borders = borders from <b>sgm_img</b>  3 For i=0 to m For j=0 to n cl = Borders[i,j]; if cl != -1 perimeter[cl] = +1 endif endFor  endFor
output  perimeter

finally, circularity can be obtained by:

$$circ = [perimeter \neq 0, \frac{area}{perimeter^2}] \quad (1)$$

To obtain cluster eccentricity, we need calculate cluster centroids and cluster principal axis as follows:

**Algorithm 2: cluster eccentricity**

## Input

Segmentation image as **sgm\_img** with dimension  $m \times n$ ;

$\text{eps} = 10^{-8}$

## Ensure

# calculate cluster centroids

1 Number\_cluster = max value from **sgm\_img** array object + 1

2 For i to m

    For j to n

$\text{cl} = \text{sgm\_img}[i,j]$

        if  $\text{cl} \neq -1$

$\text{pos}_i[\text{cl}] += i$

$\text{pos}_j[\text{cl}] += j$

        endif

    endfor

endfor

3 area = cluster\_areas(**sgm\_img**)

4  $\text{centroid}_i = \left[ \text{area} \neq 0, \frac{\text{pos}_i}{\text{area}} \right]$

5  $\text{centroid}_j = \left[ \text{area} \neq 0, \frac{\text{pos}_j}{\text{area}} \right]$

# obtain cluster principal axes

6 Perimeter = cluster\_perimeter (**sgm\_img**)

7 Borders = borders from **sgm\_img**

8 For i to m

    For j to n

$\text{cl} = \text{Borders}[i,j]$

        if  $\text{cl} \neq -1$

$\text{cxx}[\text{cl}] += (i - \text{centroid}_i[\text{cl}])^2$

$cxy[cl] += (i - centroid_i[cl]) * (j - centroid_j[cl])$ $cyy[cl] += (j - centroid_j[cl])^2$ <p>Endif</p> <p>Endfor</p> <p>Endfor</p> <p>9 <math>cxx /= [perimeter != 0]</math></p> <p><math>cxy /= [perimeter != 0]</math></p> <p><math>cyy /= [perimeter != 0]</math></p> <p>10 <math>l_1 = 0.5 * (cxx + cyy + \sqrt{(cxx + cyy)^2 - 4 * (cxx * cyy - cxy^2)})</math></p> <p>11 <math>l_2 = 0.5 * (cxx + cyy - \sqrt{(cxx + cyy)^2 - 4 * (cxx * cyy - cxy^2)})</math></p> <p># obtain eccentricity</p> <p>12 <math>Ecc = \frac{l_2}{(l_1 + eps)}</math></p>
<p>Output</p> <p>Ecc</p>

Those cluster areas, cluster circularity and cluster eccentricity were listed and named as exudates candidates. The final exudates candidates can be obtained by utilized remove operator for ‘exudates candidates’ against ‘segmentation image’. Those final exudates candidates are put (transformed) into images which will be used in next step.

**Third step** is features extraction. Several features were extracted from the exudate candidates. Those features are: orientation, max intensity, equivalent diameter, area, filled area, mean intensity, major axis length, convex area, perimeter, inertia tensor eigen values, solidity, extent, min intensity, eccentricity, minor axis length. Also, features which have dimension more than one also included, such as: moments, weighted moments hu, moments hu, inertia tensor, weighted moment central, centroid, moment central and weighted moments. The reason we chose those kinds of features is to get better characteristic of exudates. **Fourth step** is fed the statistical features to ensemble learning. 198 features were created during the feature extraction process. In the classification step, we prefer using ensemble learning due to ensemble learning were better prevents data overfitting, works relatively fast due to predictors were trained in parallel mode, and several ensemble learning based on decision tree usually can be treated as self-feature selection. Thus, due to we obtained many features (which is 198 features), we used ensemble leaning which have relation with decision tree as self-feature selection mechanisms such as: Random Forest (Breiman, 2001), XG-Boost (T. Chen & Guestrin, 2016) and META-DES (Cruz, Sabourin, Cavalcanti, & Ren, 2018). In the latter, The META-DES is ensemble methods approach where the only most competent ones are selected to classify the test sample. Even though META-DES can be used with many base classifier algorithms such as neural network, KNN and others, in this research, the candidate we are using to obtaining the competent ones is optimized random forest as base classifiers. Our proposed methods can be written as follows:

<b>Algorithm 3:</b> Exudates severity level detection methods	
Input:	Fundus image as <b>img</b>
Ensure:	<pre> # load image 1  Load and resize <b>img</b> 2  Utilized crop black border to <b>img</b> to remove background 3  Utilized CLAHE as image enhancements to <b>img</b> # exudates detection 4  Convert <b>img</b> from RGB to CIE-Luv 5  Normalized <b>img</b> 6  Utilized CLAHE to <b>img</b> 7  Normalized <b>img</b> 8  Utilized wiener filter to <b>img</b> to remove noise 9  Normalized <b>img</b> 10 Utilized canny algorithm to <b>img</b> for edge filter 11 Utilized region growing to <b>img</b> to obtain segmentation results (segmentation image) 12 Utilized clustering method to obtain the exudates candidates by considering cluster circularity, cluster areas and cluster eccentricity 13 Apply remove operator to ‘exudates candidates ’ against ‘segmentation images’ to obtain the <b>final exudates candidates</b> # extract features 14 Extract 198 features from exudates candidates # fed into ensemble learning 15 Fed into selected ensemble learning and predict the severity level </pre>
Output	Severity level with <b>img</b> of exudates candidates

## 4. Results and Discussion

### 4.1. Datasets

We used well known dataset for DR classification, such as MESSIDOR (Decencière et al., 2014) and IDRiD (Porwal et al., 2018) dataset. Both dataset aim is to diagnose the retinopathy grade from G0 which is no apparent DR, G1 is mild level DR, G2 is moderate DR, G3 is severe DR and G4 which is Proliferative DR. For detailed information about the dataset, please refer to respective papers.

### 4.2. Results

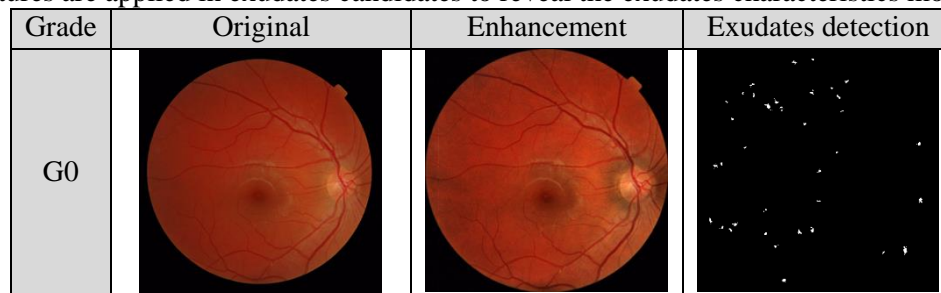
In our experiments, we applied ten-fold cross validation to reduce the randomness effects. Due to class distribution is not balance, we using SMOTE to alleviate this problem. In table 1, we described the parameter we used for this experiment. The optimum parameter was found using brute force search combination (Grid Search method). Moreover, first, we explore the effect of image enhancement methods and the effect of exudates detection using growing region and clustering with circularity, areas and eccentricity as parameters. Second, we explore the ensemble classifier which able to obtain the best performance for multi-class DR severity grade. Finally, we compared our result with several researchers in part of exudates detection.

Table 1: Base classifier ensemble parameter settings

Parameters	Values		
	Random Forest	META-DES	XG-Boost
Number Estimator	100,200,500	100,200,500	100,200,500
Max features	Automatic, square root, log2	Automatic, square root, log2	-
Max depth	4,5,6,7,8	4,5,6,7,8	4,5,6,7,8
Criterion	Gini, entropy	Gini, entropy	-
Booster	-	-	-

#### 4.2.1. Effect of Image Enhancement Methods

From Figure 2 and Figure 3, in matter of image enhancement, we can see that wiener filter and CLAHE successfully enhanced the fundus images, more characteristics of fundus images were visually revealed; in part of exudates detection, we can see the exudates detection is able to show the difference between four grades, more bigger the size of white spots frequents means the grade level is more severe. The question arise is the exudates detection in G0 (healthy subject in both of MESSIDOR and IDRiD) produce small white spots. As we checked in several results in literature from (Alzami et al., 2019; Orlando, Prokofyeva, del Fresno, & Blaschko, 2017) which the healthy fundus images also have those little spots, it means there is nothing wrong with the region growing and clustering procedures. The possible reason that there is still exist small white spots in healthy fundus images is the fundus images needs more treatment before or after obtaining the exudates candidates to filter the small white spots which produced from the exudates detection. Finally, the statistical features are applied in exudates candidates to reveal the exudates characteristics more thoroughly.



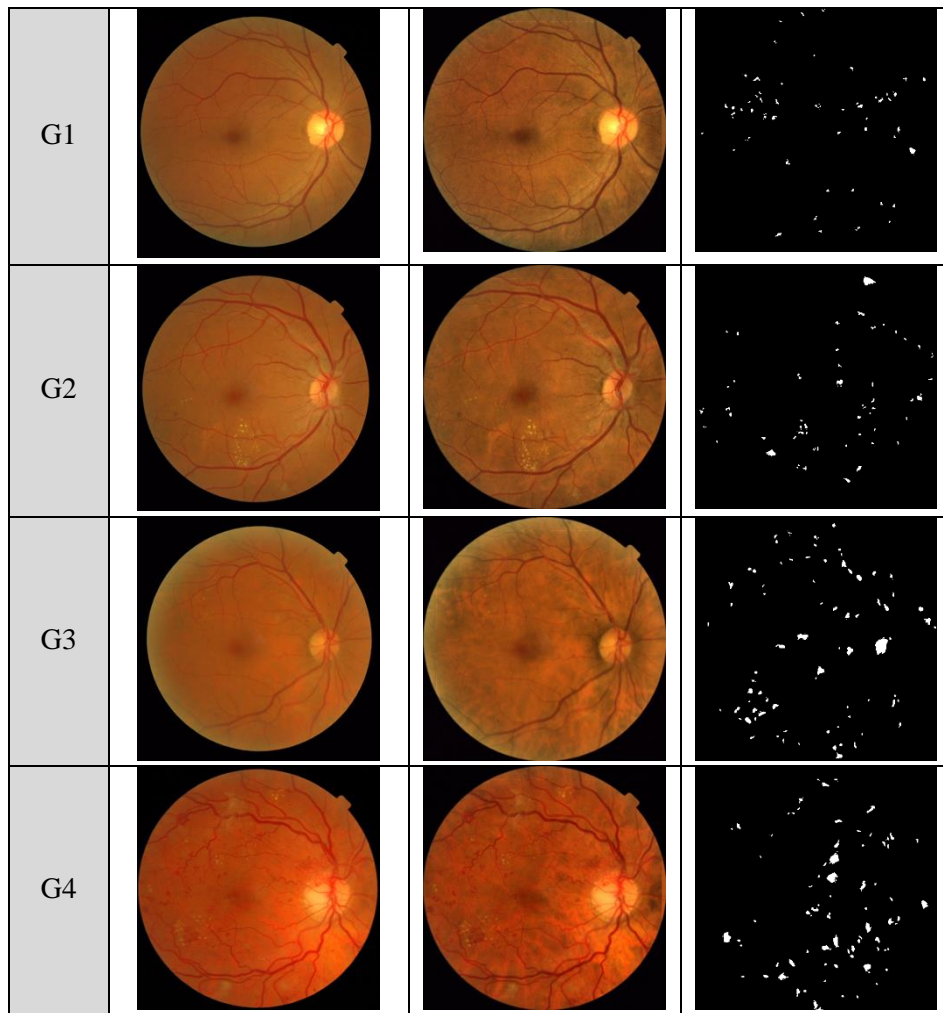
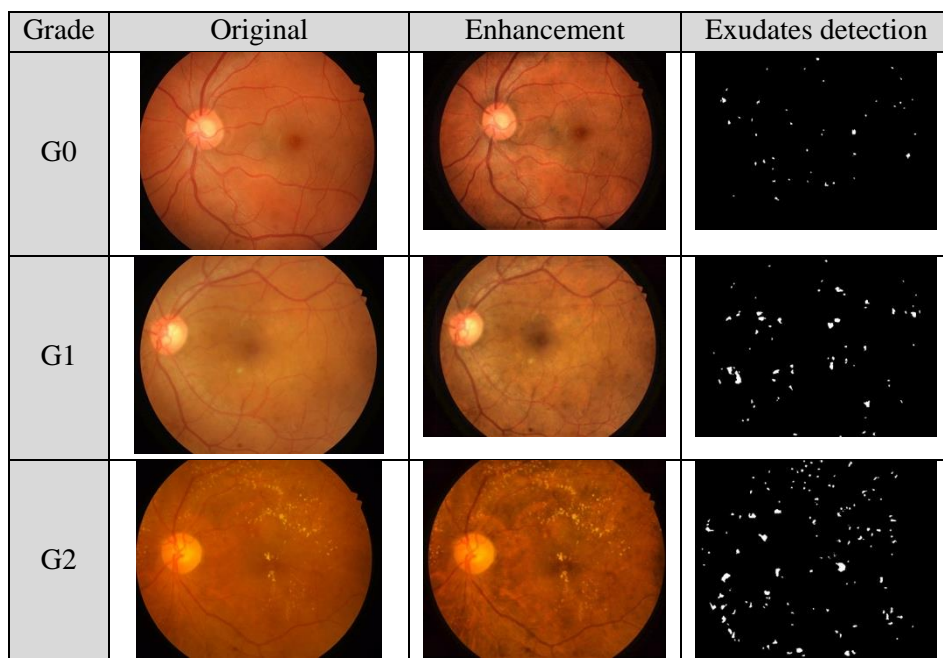


Figure 2: Exudates detection results where first column is grade level, second column is original image obtained from MESSIDOR dataset, third column is enhancement image using wiener filter and CLAHE and last column is images using exudates detection method



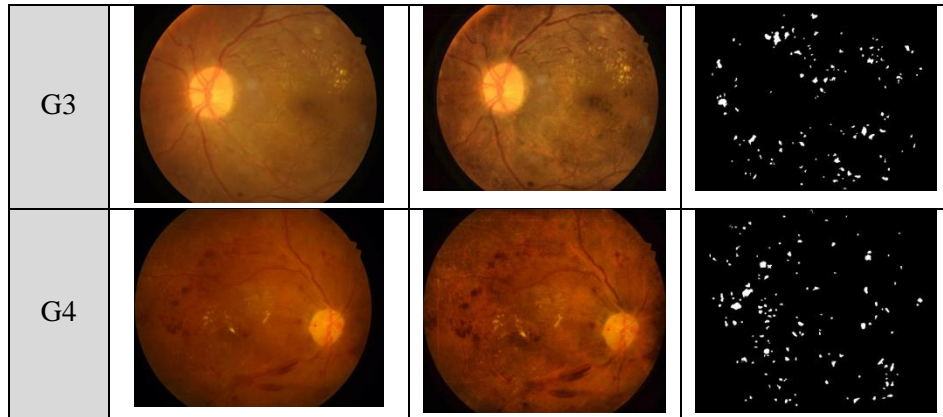


Figure 3: Exudates detection results where first column is grade level, second column is original image obtained from IDRiD dataset, third column is enhancement image using wiener filter and CLAHE and last column is images using exudates detection method

#### 4.2.2. Effects of Ensemble Classifier

With using features that we described before, we presented the ensemble classifiers performance as follows:

Table 2: Classifier performance using MESSIDOR dataset, where RF is random forest, MD is METADES and XG is XG-Boost

RF	G0	G1	G2	G3	G4	Avg
Acc	0.817	0.882	0.874	0.948	0.972	0.899±0.056
F1	0.488	0.727	0.689	0.879	0.929	0.743±0.156
MCC	0.382	0.656	0.619	0.850	0.915	0.685±0.188
MCCI	Weak	Moderate	Moderate	Strong	very Strong	
PPV	0.548	0.676	0.788	0.819	0.867	0.740±0.115
TNR	0.911	0.906	0.951	0.949	0.966	0.937±0.024
TPR	0.439	0.786	0.612	0.947	1	0.757±0.209
MD	G0	G1	G2	G3	G4	Avg
Acc	0.833	0.88	0.885	0.948	0.974	0.905±0.050
F1	0.473	0.704	0.698	0.885	0.943	0.741±0.165
MCC	0.388	0.632	0.629	0.859	0.929	0.688±0.192
MCCI	Weak	Moderate	Moderate	Strong	very strong	
PPV	0.585	0.686	0.741	0.802	0.893	0.742±0.104
TNR	0.934	0.922	0.942	0.938	0.967	0.941±0.015
TPR	0.397	0.723	0.660	0.987	1	0.754±0.224
XG	G0	G1	G2	G3	G4	Avg

Acc	0.862	0.897	0.905	0.928	0.984	0.916±0.041
F1	0.64	0.734	0.774	0.837	0.958	0.789±0.106
MCC	0.555	0.672	0.718	0.799	0.949	0.739±0.132
MCCI	Moderate	Moderate	Strong	Strong	very Strong	
PPV	0.660	0.761	0.842	0.755	0.928	0.790±0.090
TNR	0.921	0.945	0.960	0.926	0.983	0.947±0.023
TPR	0.620	0.709	0.716	0.939	0.990	0.795±0.143

Table 3: Classifier performance using MESSIDOR dataset, where RF is random forest, MD is METADES and XG is XG-Boost

RF	G0	G1	G2	G3	G4	Avg
Acc	0.817	0.952	0.764	0.841	0.941	0.8635± 0.073
F1	0.474	0.902	0.259	0.658	0.848	0.628±0.238
MCC	0.378	0.879	0.156	0.583	0.817	0.563±0.270
MCCI	Weak	Strong	Negligible	Moderate	Strong	
PPV	0.583	0.822	0.411	0.541	0.777	0.627±0.153
TNR	0.925	0.939	0.924	0.841	0.942	0.915±0.037
TPR	0.4	1	0.189	0.838	0.933	0.672±0.320
MD	G0	G1	G2	G3	G4	Avg
Acc	0.804	0.946	0.76	0.791	0.888	0.838±0.069
F1	0.463	0.88	0.25	0.584	0.698	0.575±0.213
MCC	0.355	0.850	0.131	0.479	0.630	0.489±0.244
MCCI	Weak	Strong	Negligible	Weak	Moderate	
PPV	0.558	0.814	0.36	0.471	0.690	0.579±0.160
TNR	0.915	0.944	0.910	0.7967	0.929	0.899±0.053
TPR	0.395	0.956	0.191	0.767	0.707	0.603±0.274
XG	G0	G1	G2	G3	G4	Avg
Acc	0.847	0.982	0.794	0.876	0.911	0.882±0.063
F1	0.551	0.96	0.567	0.704	0.727	0.702±0.147
MCC	0.479	0.948	0.436	0.635	0.679	0.635±0.181

MCCI	Weak	Very Strong	Weak	Moderate	Moderate	
PPV	0.695	0.947	0.522	0.625	0.8	0.718±0.146
TNR	0.948	0.984	0.842	0.892	0.964	0.926±0.052
TPR	0.457	0.972	0.621	0.806	0.666	0.704±0.174

From Table 2 and Table 3, we can conclude, that XG-Boost achieve high performance in Recall / True Positive Rate (TPR) in all class rather than Random Forest and META-DES. From the MCC itself, we can see the quality of XG-Boost is better in all class prediction rather than Random Forest and META-DES. Thus, in this section, we can conclude that by giving those statistical features, XG-Boost is able to grade the DR level by using exudates detection. For better understanding, table 2 and table 3 can be summarized in following table:

Table 4: Summarized of ensemble classifier performance using MESSIDOR and IDRiD dataset

Measurement	MESSIDOR			IDRiD		
	RF	MD	XG	RF	MD	XG
ACC	0.899	0.905	<b>0.916</b>	0.864	0.838	<b>0.882</b>
F1	0.743	0.741	<b>0.789</b>	0.629	0.575	<b>0.702</b>
MCC	0.685	0.688	<b>0.739</b>	0.563	0.490	<b>0.636</b>
PPV	0.740	0.742	<b>0.790</b>	0.627	0.579	<b>0.718</b>
TNR	0.937	0.941	<b>0.947</b>	0.915	0.899	<b>0.926</b>
TPR	0.757	0.754	<b>0.795</b>	0.672	0.604	<b>0.705</b>

#### 4.2.3. Comparison with Other Researchers

In here, we compared our method with other researchers in part of exudates detection for DR severe grading. The comparison can be seen in following table.

Table 5: Comparison with other researchers in exudates detection using MESSIDOR dataset

Researchers	Acc	Sensitivity	Specificity
Giancardo et.al (Giancardo et al., 2012)	-	0.77	0.9
Figueiredo et.al (Figueiredo, Kumar, Oliveira, Ramos, & Engquist, 2015b)	-	0.898	<b>0.974</b>
Gulshan et.al (Gulshan et al., 2016)	-	0.96	0.939
Frazao et.al (Frazao, Theera-Umpon, & Auephanwiriyaikul, 2019a)	-	0.9	0.56
Zhang et.al (Zhang et al., 2014)	-	0.623	-

Researchers	Acc	Sensitivity	Specificity
Roychowdhury et.al (Roychowdhury, Koozekanani, & Parhi, 2014)	-	<b>1</b>	0.53
Frazao et.al (Frazao, Theera-Umpon, & Auephanwiriyaikul, 2019b)	-	0.9	0.56
Kaur & Mittal (Kaur & Mittal, 2018)	0.86	0.813	0.904
Our proposed	<b>0.916</b>	0.795	0.947

From table 5, in matter of accuracy, our method obtains high performance. In other measurement, our research is comparable with another researcher. For example, Figueiredo et.al (Figueiredo et al., 2015b) obtain high sensitivity and specificity due to it using applied wavelet decomposition which helped obtain more precise in exudates detection. Roychowdhury (Roychowdhury et al., 2014) et.al which using ensemble learning obtains high sensitivity but not achieve satisfactory result in specificity. Thus, we can conclude that our research could give more insight in exudates detection researches.

### 5. Conclusion and Future works

The main highlights of the experiment as follows: first, using CIE-Luv color space, wiener filter to remove noise, canny algorithm to obtain edge and clustering to obtain the exudates candidates and normalization in every step to ensure the data distribution helps reveal the exudates candidates in visual matter. Second, XG-Boost able to grade the DR severity level better than other ensemble methods.

The conclusion from this research is: First, CIE-Luv, CLAHE in several steps, wiener filter, canny algorithm, images normalization in every step and clustering methods helps obtain the exudates candidates which can be seen visually. Then, XG-Boost successfully grading the DR severity level in multi-class problems using MESSIDOR and IDRiD dataset. Second, our methods obtain good performance and comparable with other researchers which using MESSIDOR dataset.

As we see in previous section at the figure 2 and figure 3 in part of healthy subject, the small spot intuitively should be not existing. Thus, in next research, we will consider several approaches to omit those small spots which help improve the DR severity grade classification. Also, other detection such as Microaneurysms, Hemorrhages and other will be considered in next research.

### 6. References

- Abràmoff, M. D., Reinhardt, J. M., Russell, S. R., Folk, J. C., Mahajan, V. B., Niemeijer, M., & Quèllec, G. (2010). Automated Early Detection of Diabetic Retinopathy. *Ophthalmology*, 117(6), 1147–1154. <https://doi.org/10.1016/j.ophtha.2010.03.046>
- Alzami, F., Abdussalam, Megantara, R. A., Fanani, A. Z., & Purwanto. (2019). Diabetic Retinopathy Grade Classification based on Fractal Analysis and Random Forest. *2019 International Seminar on Application for Technology of Information and Communication (ISEMANTIC)*, 272–276. <https://doi.org/10.1109/ISEMANTIC.2019.8884217>
- Alzami, F., Tang, J., Yu, Z., Wu, S., Chen, C. L. P., You, J., & Zhang, J. (2018). Adaptive Hybrid Feature Selection-Based Classifier Ensemble for Epileptic Seizure Classification. *IEEE Access*, 6, 29132–29145. <https://doi.org/10.1109/ACCESS.2018.2838559>
- Antal, B., & Hajdu, A. (2014). An ensemble-based system for automatic screening of diabetic retinopathy. *Knowledge-Based Systems*, 60, 20–27. <https://doi.org/10.1016/j.knosys.2013.12.023>
- Breiman, L. (2001). Random Forests. *Machine Learning*, 45(1), 5–32. <https://doi.org/10.1023/A:1010933404324>
- Cárdenas, J. M., Martínez-Pérez, M. E., March, F., & Hevia-Montiel, N. (2013). Mean shift based automatic detection of exudates in retinal images. In *Advances in Intelligent Systems and Computing: Vol. 184 AISC* (pp. 73–82). [https://doi.org/10.1007/978-3-642-32384-3\\_10](https://doi.org/10.1007/978-3-642-32384-3_10)
- Chen, G., Hong, Z., Guo, Y., & Pang, C. (2019). A cascaded classifier for multi-lead ECG based on feature fusion. *Computer Methods and Programs in Biomedicine*, 178, 135–143. <https://doi.org/10.1016/j.cmpb.2019.06.021>
- Chen, T., & Guestrin, C. (2016). XGBoost: A scalable tree boosting system. *Proceedings of the ACM SIGKDD International Conference on Knowledge Discovery and Data Mining, 13-17-Aug, 785–794*. <https://doi.org/10.1145/2939672.2939785>
- Cruz, R. M. O., Sabourin, R., Cavalcanti, G. D. C., & Ren, T. I. (2018). {META-DES:} {A} Dynamic Ensemble Selection Framework using Meta-Learning. *CoRR*, abs/1810.0. Retrieved from <http://arxiv.org/abs/1810.01270>
- Decencièrè, E., Zhang, X., Cazuguel, G., Laÿ, B., Cochener, B., Trone, C., ... Klein, J. C. (2014). Feedback on a

- publicly distributed image database: The Messidor database. *Image Analysis and Stereology*, 33(3), 231–234. <https://doi.org/10.5566/ias.1155>
- Figueiredo, I. N., Kumar, S., Oliveira, C. M., Ramos, J. D., & Engquist, B. (2015a). Automated lesion detectors in retinal fundus images. *Computers in Biology and Medicine*, 66, 47–65. <https://doi.org/10.1016/j.compbiomed.2015.08.008>
- Figueiredo, I. N., Kumar, S., Oliveira, C. M., Ramos, J. D., & Engquist, B. (2015b). Automated lesion detectors in retinal fundus images. *Computers in Biology and Medicine*, 66, 47–65. <https://doi.org/10.1016/j.compbiomed.2015.08.008>
- Fleming, A. D., Goatman, K. A., Philip, S., Williams, G. J., Prescott, G. J., Scotland, G. S., ... Scottish Diabetic Retinopathy Clinical Research Network. (2010). The role of haemorrhage and exudate detection in automated grading of diabetic retinopathy. *The British Journal of Ophthalmology*, 94(6), 706–711. <https://doi.org/10.1136/bjo.2008.149807>
- Fraz, M. M., Jahangir, W., Zahid, S., Hamayun, M. M., & Barman, S. A. (2017). Multiscale segmentation of exudates in retinal images using contextual cues and ensemble classification. *Biomedical Signal Processing and Control*, 35, 50–62. <https://doi.org/10.1016/j.bspc.2017.02.012>
- Fraza, L. B., Theera-Umpon, N., & Auephanwiriyakul, S. (2019a). Diagnosis of diabetic retinopathy based on holistic texture and local retinal features. *Information Sciences*, 475, 44–66. <https://doi.org/10.1016/j.ins.2018.09.064>
- Fraza, L. B., Theera-Umpon, N., & Auephanwiriyakul, S. (2019b). Diagnosis of diabetic retinopathy based on holistic texture and local retinal features. *Information Sciences*, 475, 44–66. <https://doi.org/10.1016/j.ins.2018.09.064>
- Giancardo, L., Meriaudeau, F., Karnowski, T. P., Li, Y., Garg, S., Tobin, K. W., & Chaum, E. (2012). Exudate-based diabetic macular edema detection in fundus images using publicly available datasets. *Medical Image Analysis*, 16(1), 216–226. <https://doi.org/10.1016/j.media.2011.07.004>
- Gulshan, V., Peng, L., Coram, M., Stumpe, M. C., Wu, D., Narayanaswamy, A., ... Webster, D. R. (2016). Development and Validation of a Deep Learning Algorithm for Detection of Diabetic Retinopathy in Retinal Fundus Photographs. *JAMA*, 316(22), 2402. <https://doi.org/10.1001/jama.2016.17216>
- Harangi, B., & Hajdu, A. (2014). Automatic exudate detection by fusing multiple active contours and regionwise classification. *Computers in Biology and Medicine*, 54, 156–171. <https://doi.org/10.1016/j.compbiomed.2014.09.001>
- Hosseini, M.-P., Pompili, D., Elisevich, K., & Soltanian-Zadeh, H. (2018). Random ensemble learning for EEG classification. *Artificial Intelligence in Medicine*, 84, 146–158. <https://doi.org/10.1016/j.artmed.2017.12.004>
- Kaur, J., & Mittal, D. (2018). A generalized method for the segmentation of exudates from pathological retinal fundus images. *Biocybernetics and Biomedical Engineering*, 38(1), 27–53. <https://doi.org/10.1016/j.bbe.2017.10.003>
- Li, H., & Chutatape, O. (2004). Automated Feature Extraction in Color Retinal Images by a Model Based Approach. *IEEE Transactions on Biomedical Engineering*, 51(2), 246–254. <https://doi.org/10.1109/TBME.2003.820400>
- Liu, Q., Zou, B., Chen, J., Ke, W., Yue, K., Chen, Z., & Zhao, G. (2017). A location-to-segmentation strategy for automatic exudate segmentation in colour retinal fundus images. *Computerized Medical Imaging and Graphics*, 55, 78–86. <https://doi.org/10.1016/j.compmedimag.2016.09.001>
- Mondéjar-Guerra, V., Novo, J., Rouco, J., Penedo, M. G., & Ortega, M. (2019). Heartbeat classification fusing temporal and morphological information of ECGs via ensemble of classifiers. *Biomedical Signal Processing and Control*, 47, 41–48. <https://doi.org/10.1016/j.bspc.2018.08.007>
- Mookiah, M. R. K., Acharya, U. R., Chua, C. K., Lim, C. M., Ng, E. Y. K., & Laude, A. (2013). Computer-aided diagnosis of diabetic retinopathy: A review. *Computers in Biology and Medicine*, 43(12), 2136–2155. <https://doi.org/10.1016/j.compbiomed.2013.10.007>
- Mursalin, M., Zhang, Y., Chen, Y., & Chawla, N. V. (2017). Automated epileptic seizure detection using improved correlation-based feature selection with random forest classifier. *Neurocomputing*, 241, 204–214. <https://doi.org/10.1016/j.neucom.2017.02.053>
- Niemeijer, M., Abramoff, M. D., & van Ginneken, B. (2009). Information fusion for diabetic retinopathy CAD in digital color fundus photographs. *IEEE Transactions on Medical Imaging*, 28(5), 775–785. <https://doi.org/10.1109/TMI.2008.2012029>
- Orlando, J. I., Prokofyeva, E., del Fresno, M., & Blaschko, M. B. (2017). Convolutional neural network transfer for automated glaucoma identification. *12th International Symposium on Medical Information Processing and Analysis*, 10160, 101600U. <https://doi.org/10.1117/12.2255740>
- Pizer, S. M., Amburn, E. P., Austin, J. D., Cromartie, R., Geselowitz, A., Greer, T., ... Zuiderveld, K. (1987). Adaptive histogram equalization and its variations. *Computer Vision, Graphics, and Image Processing*, 39(3), 355–368. [https://doi.org/10.1016/S0734-189X\(87\)80186-X](https://doi.org/10.1016/S0734-189X(87)80186-X)
- Porwal, P., Pachade, S., Kamble, R., Kokare, M., Deshmukh, G., Sahasrabudhe, V., & Meriaudeau, F. (2018). Indian Diabetic Retinopathy Image Dataset (IDRiD): A Database for Diabetic Retinopathy Screening Research. *Data*, 3(3), 25. <https://doi.org/10.3390/data3030025>

- Roychowdhury, S., Koozekanani, D. D., & Parhi, K. K. (2014). DREAM: Diabetic Retinopathy Analysis Using Machine Learning. *IEEE Journal of Biomedical and Health Informatics*, 18(5), 1717–1728. <https://doi.org/10.1109/JBHI.2013.2294635>
- Shaw, J. E., Sicree, R. A., & Zimmet, P. Z. (2010). Global estimates of the prevalence of diabetes for 2010 and 2030. *Diabetes Research and Clinical Practice*, 87(1), 4–14. <https://doi.org/10.1016/j.diabres.2009.10.007>
- Usman Akram, M., Khalid, S., Tariq, A., Khan, S. A., & Azam, F. (2014). Detection and classification of retinal lesions for grading of diabetic retinopathy. *Computers in Biology and Medicine*, 45, 161–171. <https://doi.org/10.1016/j.combiomed.2013.11.014>
- Zhang, X., Thibault, G., Decenci ere, E., Marcotegui, B., La y, B., Danno, R., ... Erginay, A. (2014). Exudate detection in color retinal images for mass screening of diabetic retinopathy. *Medical Image Analysis*, 18(7), 1026–1043. <https://doi.org/10.1016/j.media.2014.05.004>



This work is licensed under a Creative Commons Attribution Non-Commercial 4.0 International License.